Journal of the Korean Vacuum Science & Technology; JKVST
Vol.6, No.3, 2002, pp.126~132

Leakage Current Mechanism of Thin-Film Diode for Active-Matrix Liquid Crystal Displays

Myung Jae Lee†, Kwan Soo Chung, and Dong-Sik Kim*

Dept. of Electronics Engineering, Kyung-Hee University, Suwon, Kyunggi, Korea
**Dept. of Computer Engineering, Inha Technical College, Inchon, Korea*
(Received July 10, 2001)

Abstract

The origin of image-sticking in metal-insulator-metal type thin-film diode liquid crystal displays(TFD-LCDs) is the asymmetric current-voltage(I-V) characteristic of TFD element. We developed that TFD-LCDs have reduced-image-sticking. Tantalum pentoxide(Ta_2O_5) is a candidate for use in metal-insulator-metal(MIM) capacitors in switching devices for active-matrix liquid crystal displays(AM-LCDs). High quality Ta_2O_5 thin films have been obtained from anodizing method. We fabricated a TFD element using Ta_2O_5 films which had perfect current-voltage symmetry characteristics. We applied novel process technologies which were postannealed whole TFD element instead of conventional annealing to the fabrication. One-Time Post-Annealing(OPTA) heat treatment process was introduced to reduce the asymmetry and shift of the I-V characteristics, respectively. OPTA means that the whole layers of lower metal, insulator, and upper metal are annealed at one time. Futhermore, in this paper, we discussed the effects of top-electrode metals and annealing conditions.

1. Introduction

In recent years, active-matrix liquid-crystal displays (AM-LCD) hane been widely used in a variety of applications. In comparison with thin-film transistor liquid-crystal displays(TFT-LCDs), metal-insulator-metal liquid-crystal displays(MIM-LCDs) has a lot of advantages such as simple process, lower cost, lower power consumption, and larger aperture ratio, etc. However, the most serious problem of the MIM-LCDs is image-sticking(long time image-retention). The phenomena are caused by the asymmetry of the current-voltage(I-V) characteristics of the MIM devices. Several researches have been performed to overcome the problem by improving the structure of MIM device and the materials of insulating layer [1,2]. As a result, tandem structure was proposed. The structure of tandem is composed of two MIM and two electrical paths for symmetry. But, it is not desirable because the tandem structure is very complicated and, therefore, causes high threshold voltage, poor reliability and high cost of fabrication.

In this work, we attempted new processes of our unique multi-step anodization(MSA) and one-time post annealing (OTPA) treatment. The new processes were applied to the fabrication of a high performance MIM-LCDs with perfect symmetry and uniformity. All the fabrication processes were developed below 150℃ so as to allow the application of plastic substrates.

The electrical conduction of anodized Ta_2O_5 films have been investigated in order to improve the asymmetry [4-6]. The TFD element with a Cr/Ta_2O_5/Ta or Ti/Ta_2O_5/Ta type MIM diode was chosen and studied. Anodized Ta_2O_5 was made between 20 nm and 70 nm thick from ~200 nm tantalum films sputter deposited on glass

† E-mail : lmj1@khu.ac.kr

substrates. After fabricated MIM, the whole MIM elements were annealed in vacuum at various temperatures. We report the experimental results that the I-V asymmetric characteristics depends on the material of the top-electrode of MIM elements as well as on the heat-treatment temperatures and the conduction mechanism of the I-V asymmetry [7-12].

2. Experimental

MIM structures were fabricated to evaluate the electrical properties of the Ta_2O_5 films. First, the Ta film was deposited on a glass substrate to a thickness of 200 nm by using dc magnetron sputtering in an Ar ambient. The pressure of the reaction chamber was maintained at 5 mTorr, and the substrate was at room temperature. The Ta film was patterned by using a photo-engraving process(PEP) and was then partially anodized. The anodization was performed in 1.0 wt.% aqueous ammonium tartrate solution with a silicon wafer counter electrode, and the solution temperature was 25℃. A constant current(1 mA/cm^2) was applied to the samples until the desired voltage was reached. The thickness of the Ta_2O_5 layer was linearly related to the final anodization voltage with a proportionality constant of approximately 14.7 Å/V at room temperature. The thickness of each Ta_2O_5 layer and its refractive index were measured with an ellipsometer at 633 nm, assuming zero extinction. The measured indices of refraction were 2.15±0.05. Next, as a counter-electrode, a Cr or a Ti film was deposited on the Ta_2O_5/Ta array to a thickness of 200 nm by RF sputtering in Ar gas and was patterned by using a PEP.

The electrical characteristics of the Ta_2O_5 films were studied as functions of the electric field and the temperature(150~400℃). An HP4145B semiconductor parameter analyzer pA meter was used to measure the current-voltage(I-V) characteristics and the breakdown voltage. The breakdown voltage was defined as the current compliance of the instrument, which was 4×10^{-2} A. The interface was investigated using transmission electron microscopy(TEM).

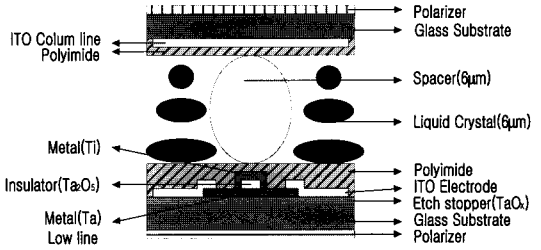

(a) cross-sectional view of a MIM-LCD panel

(b) Photograph of the MIM matrix

Fig. 1. TFD configuration.

The structure of a TFD element is shown in Fig. 1. The element consisted of a pair of Ta and Ti or Cr metal films with a Ta_2O_5 film inserted between the metal films. The thicknesses of the Ti, Ta_2O_5, and Ta films were 200 nm, 20~60 nm, and 200 nm, respectively. The TFD element size was 20 μm×20 μm.

3. Results and Discussion

3.1 Investigation of Microstructure in Ta_2O_5 Thin Films.

The thicknesses of the deposited Ta_2O_5 films were determined by using both an ellipsometer and a thickness profile meter with α-step. Refractive indices were about 2.1 for as-deposited Ta_2O_5 films and about 2.1 - 2.2 for thermally treated Ta_2O_5 films; thicknesses ranged from 200 to 1000 Å. In addition, Rutherford back-scattering (RBS) observations were taken to examine the compositions of the oxide films. Fig. 2 depicts a RBS profile. The observation shows the spectrum of 2-MeV He ions back-scattered from the oxide film at an 80° tilting angle. The straight line shows the simulated results for a standard Ta_2O_5 film, and the dotted line shows the spectrum

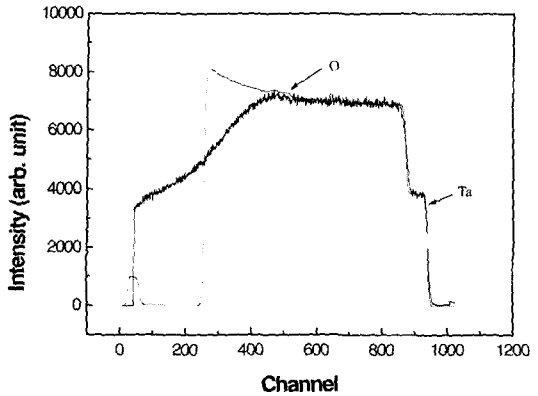

Fig. 2. RBS profiles of Ta_2O_5 film(750 Å) anodized on Ta thin film(4000 Å) deposited on Si substrate.

of the anodized oxide film. The measured spectrum coincided with the simulated results, and no differences between the as-deposited Ta_2O_5 film and thermally treated Ta_2O_5 films were observed in this experiment. Therefore, we conclude that the oxide films(TaO_X) obtained from the anodizing process at an anodizing voltage of 48 V are reliable Ta_2O_5 films with a 750-Å thickness.

3.2 Effects of postannealing on Current-Voltage Characteristics

The fabricated MIM element was annealed at 150 ~450℃ for 2h in a vacuum. The electrode annealing seemed to a key process that affected the electrical properties since the interface states between the Ta_2O_5 and both electrodes constituted a portion of the leakage current. The reasons for increasing current density with increasing annealing temperature are thought to be reduced the barrier heights [12] of the interfaces between the Ta_2O_5 layer and the two electrodes. Fig. 3 shows the energy band diagrams of the TFD element before and after annealing. In regions (2) and (4) of Fig. 3(b), the metal, which is excessive in the oxide film, behaves as a dopant and carrier density is probably very high. In this situation, the Fermi level is located within the conduction band, and regions (2) and (4) are considered to be degenerate. Fig. 3 also, suggests that the thickness of the interface layer increases with increasing annealing temperature. As shown in the TEM image of Fig. 4, after 350℃ annealing of the whole TFD element for 2h in a vacuum, new layers, regions (2) and (4), appear. The leakage current increases with increasing annealing temperature as shown in Fig. 5. In order to improve current-voltage symmetry characteristics of MIM devices, we suggest postannealing of the whole TFD element. As shown in Fig. 6, a high-performance MIM device with perfect symmetry could be achieved by using

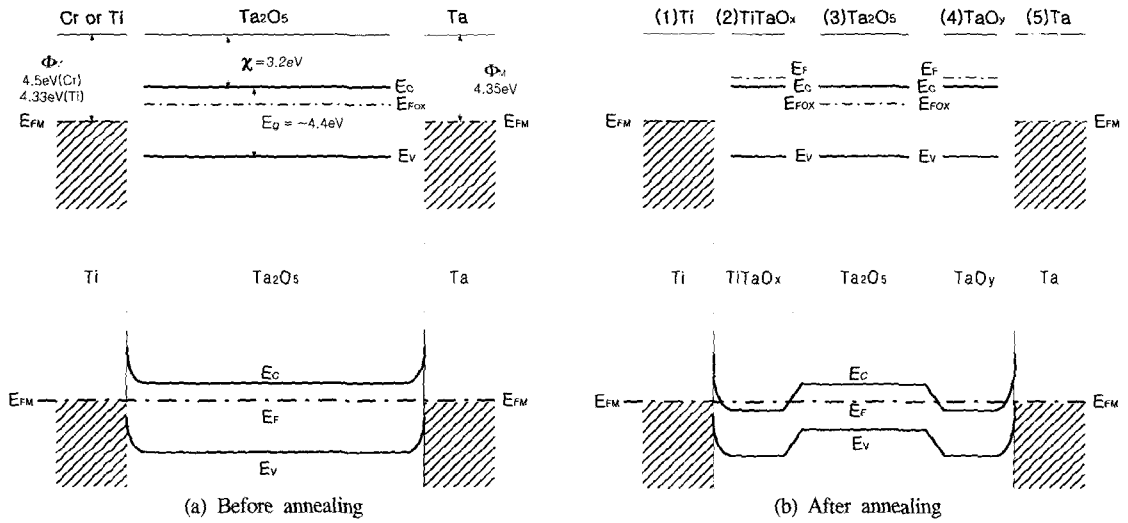

Fig 3. Energy band diagram of TFD element.

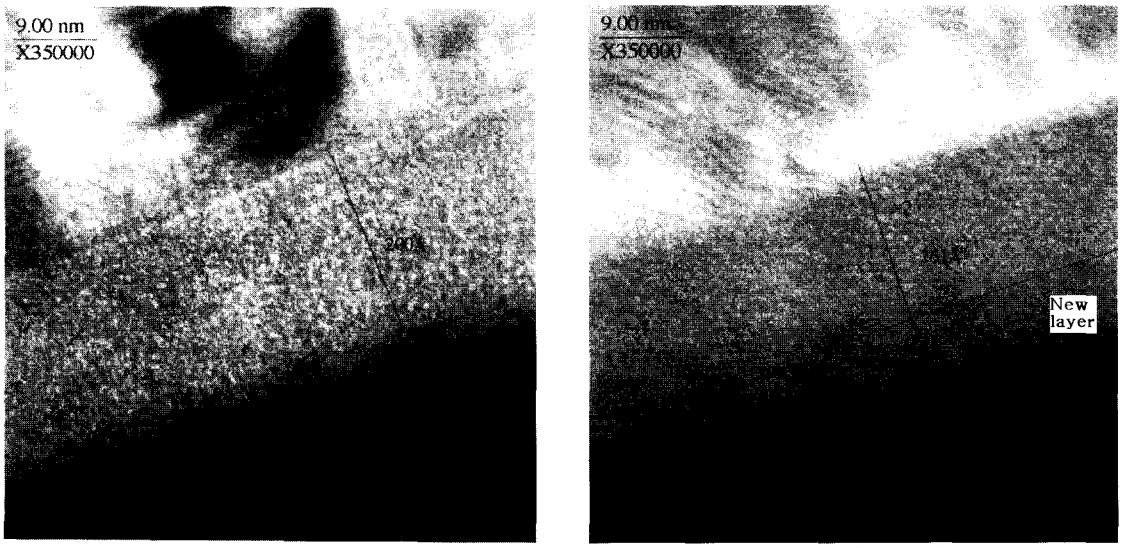

(a) Not annealing (b) After 350℃ annealing

Fig. 4. cross-sectional TEM image of Ta_2O_5.

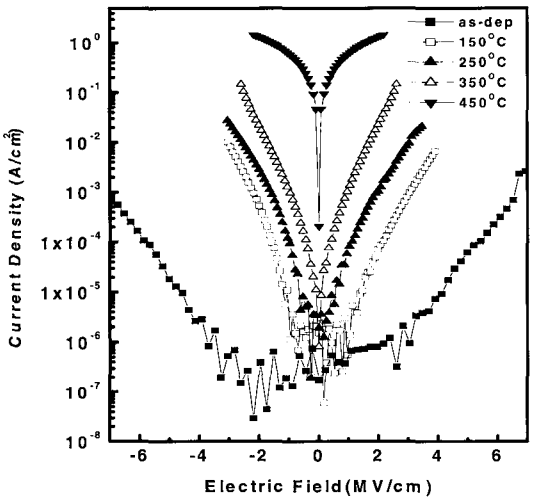

Fig. 5. I-V Characteristics for anodized Ta_2O_5 film of 610 Å thickness as annealing temperature.

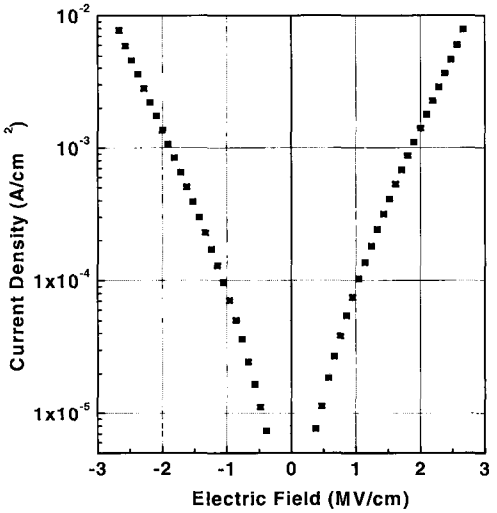

Fig. 6. I-V Characteristics of the TFD element with top electrode Ti.

novel technologies and a TFD element with a Ti/Ta_2O_5/Ta element annealed at 350℃ for 2h in a vacuum. This device exhibited an acceptable low leakage current density(below 10^{-7} A/cm^2 at 2 MV/cm), a reasonable breakdown voltage(5 - 7 MV/cm) and a high dielectric constant(23 - 29).

3.3 Conduction mechanisms of TFD element with Ta_2O_5

The leakage current in a dielectric film can be due to several conduction mechanisms, including Schottky emission [8], Poole-Frenkel emission [11,12], Fowler-

Nordheim tunnelling and space-charge-limited current (SCLC) [13]. Electronic conduction in a thin Ta_2O_5 film has been interpreted in terms of electronic conduction theories. A perennial problem is the question whether the dc conduction is controlled by a Schottky emission (SE electrode-limited conduction) or by a Poole-Frenkel (PF, bulk-limited conduction) mechanism. Schottky emission is described by [8]

$$J_{SE} = AT^2 \exp\left[\frac{q\left(-\Phi_B + \sqrt{qE/4\pi\varepsilon_i}\right)}{kT}\right] \quad (1)$$

and Poole-Frenkel emission by [8]

$$J_{PE} = C\,E \exp\left[\frac{q\left(-\Phi_i + \sqrt{qE/\pi\varepsilon_i}\right)}{kT}\right] \quad (2)$$

where J is the current density(A/cm^2), A is the Richardson constant, which is equal to 120 A/cm^2-K^2, T denotes the absolute temperature, q is the elementary electric charge, k represents the Boltzmann constant, C is a constant, E represents the electric field, Φ_B is barrier height, Φ_i is the depth of the donor level of the oxide, and ε_i is the insulator dielectric constant of the oxide.

The interpretation of conduction mechanisms from the experimental data has been done by using the measured slope of the log(J) vs $E^{1/2}$ and log(J/E) vs $E^{1/2}$ plots. If the measured value of log(J) vs $E^{1/2}$ is linear, the conduction mechanism is considered to be a SE(electrode-limited) process. On the other hand, if the measured value of log(J/E) vs $E^{1/2}$ is linear, the conduction mechanism is considered to a PF(bulk-limited)process. Fig. 7 shows the leakage current density vs applied electric field for a MIM capacitor with the top Ti electrode. Fig. 8 plots the logarithmic current density as a function of the square root of the electric field [log(J) vs $E^{1/2}$]. Under a low electric field (< 2.2 MV/cm), a straight line can be obtained. The dominant conduction mechanism at low fields is, therefore, determined to be Schottky emission.

The electrical conduction is governed by a different mechanism at higher electric fields. Fig. 9 plots the logarithmic current density divided by the electric field as a function of the square root of the electric field [log(J/E) vs $E^{1/2}$]. The curve is a straight line at high electric fields (> 2.2 MV/cm^2). Therefore, the dominant

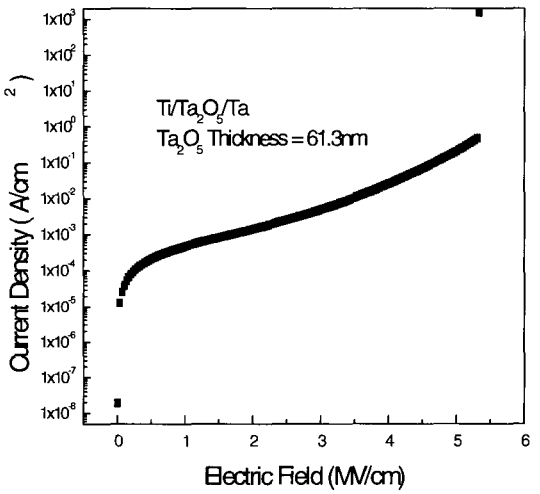

Fig. 7. I-V Characteristics of a MIM diode with the top Ti electrode biased positive at 150℃ annealing for 2h in vacuum. The size of the MIM is 20 ㎛ ×20 ㎛.

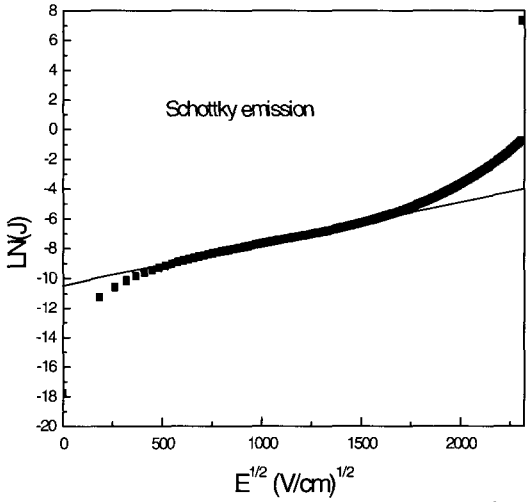

Fig. 8. The ln(J) is plotted as a function of $E^{1/2}$ of fig. 2 for the amorphous tantalum oxide MIM diode. The straight line behavior at low electric field(< 2.2 MV/cm)indicates Schottky emission mechanism.

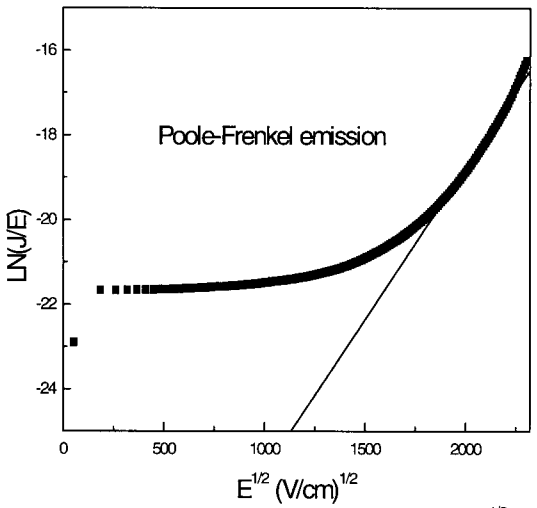

Fig. 9. The ln(J/E) is plotted as a function of $E^{1/2}$ of fig. 2 for the tantalum oxide MIM diode. The straight line behavior at high electric field(2.2 - 5.2 MV/cm) indicates Poole Frenkel conduction mechanism.

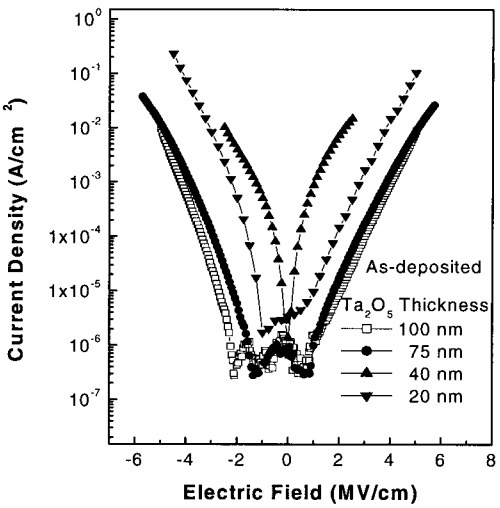

Fig. 10. I-V characteristics of TFD element for different thickness of Ta_2O_5 at as-deposited.

conduction mechanism in this high field range is considered to be a Poole-Frenkel conduction mechanism.

3.4 Conduction mechanisms of TFD element with Ta_2O_5 films as oxide thickness

Voltages and fields are plotted with respect to the sign of the voltage on the top electrode. The terms "forward" and "reverse" bias refer to positive and negative voltages on the top electrode, respectively. We observed large I-V asymmetric characteristics in thin films, defined here to be films thinner than 250 Å. Depending on the top material, the I-V characteristics had different threshold voltages at the same Ta_2O_5 thickness(230 Å). This implied that the electrode-limited process dominated the bulk-limited process. Therefore, the dominant conduction mechanism for thin films was the Schottky conduction mechanism. As shown in Fig. 10, we observed the lowest leakage currents in thick films (>300 Å). Also, Fig. 10 shows that the voltage sign has less effect on the leakage current than it did for thin films. Therefore, the thicker the films is, the more effective Poole-Frenkel emission(bulk-limited) is.

4. Conclusion.

In this work we successfully deposited Ta_2O_5 thin films by anodic oxidation and investigated the electrical and physical characteristics. Using these Ta_2O_5 thin films, high performance 2 ″ TFD-LCD was fabricated. As shown in Fig. 11, the switching operation of the TFD-LCD was very uniform. We have identified two types of conduction mechanism in Ta_2O_5 films. Schottky emission is dominant conduction mechanism at low electric field below 2.2 MV/cm, and Poole Frenkel emission is dominant at high field above 2.2 MV/cm. Also, we concluded that Schottky emission was associated with thin films(< 300 Å) than thick films(> 300 Å) since we observe that the leakage current was largely affected by both interface states in the thin film Ta_2O_5 (< 300 Å).

Reference

[1] A. G. Revesz and T. D. Kirkendall, J. Electrochem. Soc. **123**, 1515 (1976).

[2] G. S. Oehrlein and A. Reisman, J. Appl. Phys. **54**, 6502 (1983).

[3] K. Ohta, K. Yamada, R. Shmizu, and Y. Tarui,

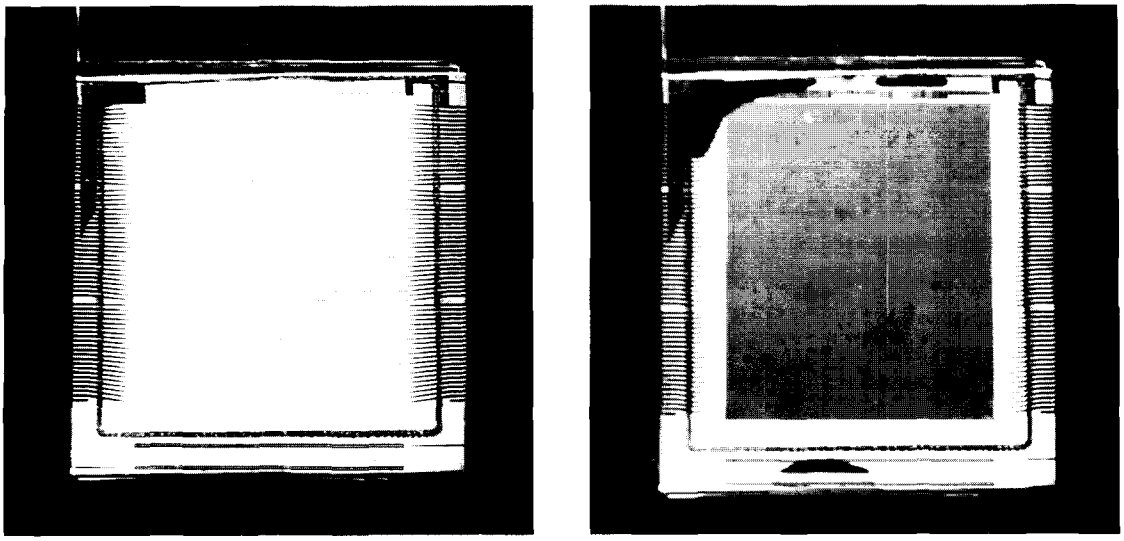

(a) ON-State (b) OFF-State

Fig. 11. 2-inch TFD-LCD switching operation.

IEEE Trans. Electron. Devices ED-29 368 (1982).

[4] Y. Nishioka, S . Kimura, and K. Mukai, Proceedings of the 165th Electrochemical Society Meeting p. 160 (1984).

[5] H. Shinriki and M. Nakata, IEEE Trans. Electron. Devices ED-38, 455 (1991).

[6] R. A. B. Devine, L. Vallier, J. L. Autran, P. Paillet, and J. L. Leray, Appl. Phys. Lett. **68** (1996) 1775.

[7] T. Hirai, H. Morita, and M. Tasaka, Jpn. J. Appl. Phys. **38**, 5287 (1999).

[8] M. Ohring, "The Materials Sciencd of Thin Films" (Academic Press, San Diego,1992

[9] R. M. Fleming, D. V. Lang, and C. D. W. Jones *et al.*, J. Appl. Phys. **88**, 850 (2000).

[10] J. G. Simmons, J. Phys. D. Appl. Phys. **4**, 613 (1971).

[11] J. Frenkel, Phys. Rev. **54**, 647 (1938).

[12] J. Frenkel, Tech. Phys. **5**, 685 (1938).

[13] R. A. B. Devine, L. Vallier, J. L. Autran, P. Paillet, and J. L. Leray, Appl. Phys. Lett. **68**, 25 (1996).

[14] D. E Castleberry: IEEE Trans. Electron Devices **26**, 1123 (1979).

[15] D. R. Baraff, J. R. Long, B. K. McLaurin, C. J. Miner, and R. W. Streter: IEEE Trans. Electron Devices **28**, 736 (1981).

[16] T. Hirai, K. Miyake, T. Nakamura, S. Kamagami, and H. Morita, Jpn. J. Appl. Phys. **31**, 4582 (1992)

[17] H. Morita, S. Kamagami, Y. Abe, T. Hirai, M. Watanabe, K. Miyake, T. Nakamura and J. Hirota: Eurodisplay'93 Late-News Papers (1993), p. 597.